LETTER TO THE EDITOR

Neutron production from picosecond laser irradiation of deuterated targets at intensities of 1.4×10^{19} W cm^{-2}

Plasma Phys. Control. Fusion **40** (1998) 175–182. Printed in the UK PII: S0741-3335(98)88548-5

LETTER TO THE EDITOR

Neutron production from picosecond laser irradiation of deuterated targets at intensities of 10^{19} W cm^{-2}

P A Norreys†, A P Fews‡, F N Beg§, A R Bell§, A E Dangor§, P Lee§, M B Nelson‖, H Schmidt¶, M Tatarakis§ and M D Cable‖

† Central Laser Facility, Rutherford Appleton Laboratory, Chilton, Didcot, Oxon OX11 0QX, UK

‡ H H Wills Physics Laboratory, University of Bristol, Tyndall Avenue, Bristol BS8 1TL, UK

§ Blackett Laboratory, Imperial College of Science Technology and Medicine, Prince Consort Road, London SW7 2BZ, UK

‖ University of California, Lawrence Livermore National Laboratory, Livermore, California 94550, USA

¶ Institut fuer Plasmaforschung, Universitaet Stuttgart, Pfaffenwaldring 31, 70569 Stuttgart, Germany

Received 22 October 1997, in final form 18 November 1997

Abstract. Neutron fluxes of up to 7×10^7 neutrons/sr were measured when planar deuterated targets were irradiated with 1.3 ps FWHM (full width at half maximum) laser pulses at a wavelength of 1054 nm and focused intensities up to 10^{19} W cm^{-2}. The neutron energy spectra are consistent with an angularly dispersed beam target interaction, whereas a thermonuclear source is considered unlikely.

The fast ignitor scheme for inertial confinement fusion (ICF) has recently been proposed [1]. In this scheme, short-pulse, high-intensity laser radiation creates energetic electrons at the critical density surface of an already compressed high-density plasma. These electrons are transported into the deuterium–tritium fuel and heat it to thermonuclear temperatures before it has time to disassemble. There is a considerable saving of laser drive energy as the creation of a hot spark at the centre of the compressed fuel is no longer required, and the laser symmetry requirements can be significantly relaxed. For this scheme, fundamental experiments need to be carried out to characterize the generation of fast electrons and ions, and their associated energy transport throughout the target.

Measurements of the number of fast electrons and their characteristic temperature can be achieved by the established technique of K_α spectroscopy [2]. However, measurement of fast ion transport is complicated by the extremely strong electrostatic fields that are generated. Ion measurements made outside the target will be characteristic not of their behaviour in the plasma during the interaction, but of the expansion of the plasma, which is driven by the fast electrons [3]. Thus to determine the fast ion behaviour in the plasma during the interaction, other more direct diagnostics need to be used.

Position sensitive neutron spectroscopy is just such a technique. Energetic deuterons, created during the interaction of a high-intensity laser pulse, produce neutrons as a result of collisions, either thermally or by a beam target (high-energy ion incident on a relatively slow ion) type interaction. Neutron measurements in the forward and backward directions

0741-3335/98/020175+08$19.50

are a very sensitive measure of any systematic motion of the centre of mass of the reacting ions and will register either as an upshift or downshift in neutron energy, depending on the position of the detector. The technique should differentiate between ion motion into and out of the target: 2.5-dimensional particle-in-cell (PIC) calculations predict that a substantial percentage of the laser energy is transferred to ions directed into the plasma [4]. Similarly, position sensitive neutron spectroscopy can differentiate between fast ions impacting deuterons deposited on both diagnostic equipment and the walls of the vacuum vessel [5].

The experimental configuration used was similar to that used in other experiments at the Rutherford Appleton Laboratory [6, 7]. The VULCAN laser, operating at a wavelength of 1.054 μm, gave pulses of 1.3 ps duration [8]. An equivalent plane monitor showed the laser was focused to a 12–15 μm focal spot. An off-axis parabolic mirror of 44 cm focal length focused between 8–20 J of p-polarized laser radiation at 30° angle of incidence onto either a massive flat deuterated polystyrene (C_8D_8) target of $\sim$120 μm thickness, or onto a cryogenically cooled deuterium pellet of 1 cm diameter and 5 mm thickness.

The neutron diagnostics consisted of current mode time-of-flight detectors, silver activation counters and γ-ray insensitive CR-39 plastic nuclear track detectors. The current mode time-of-flight detectors comprised a scintillator/photomultiplier combination and were based on the Lawrence Livermore National Laboratory (LLNL) design [9]. They were located behind the target outside the chamber at a distance of 1.21 m at 145° from the target normal, and at 1.18 m in front of the target in the target normal direction at 0°. On some shots, the time-of-flight detector located behind the target was moved to the 0° position at a distance of 1.96 m. The activation counters were placed at a distance of 1 m from the target at 20°.

The CR-39 detectors were covered in 3 mm of lead to stop all energetic charged particles from the plasma impinging on the detector. The lead filter has a negligible effect on the transmission of neutrons with energies between 1 and 4 MeV. The neutrons can then be detected by observing the knock-on protons in the CR-39. CR-39 records charged nuclear particles as tracks which are etched into the surface of the detector after exposure. Each incident ion produces a separate etch track, the dimensions and depth of penetration of which enable the energy and the atomic number of the fast ions to be individually determined [10]. In this way, neutrons of a particular energy produce a characteristic distribution of proton track size which is different from that of neutrons of a different energy. These distribution shapes are extremely sensitive to the incident neutron energies of $\leqslant$3 MeV. A maximum entropy unfolding technique, similar to that used in image deconvolution [11] is then applied to the recorded track size distribution to produce a neutron spectrum. This technique selects the optimum neutron spectrum by matching a predicted track size distribution to the measured data. The spectrum which is produced is the flattest (maximum entropy) neutron distribution where the measured and predicted proton distributions are consistent with each other. The resulting spectrum will then only contain those significant features which are required to fit the predicted proton track distribution to the measured data. The neutron spectrum derived from the maximum entropy unfolding technique are limited to energies up to 3 MeV due to the progressive reduction in track size of the knock-on protons for higher neutron energies. The detectors were calibrated against a test exposure of a known 2.5 MeV neutron flux from the National Physical Laboratory, UK.

Yields in the range 8×10^6–7×10^7 neutrons/sr for C_8D_8 and D_2 targets were measured by the track detectors and confirmed by the activation counters. Figure 1 shows a neutron spectrum calculated by unfolding the proton distribution by the maximum entropy method described above for a C_8D_8 irradiated target. Figure 1(a) shows the spectrum from detectors

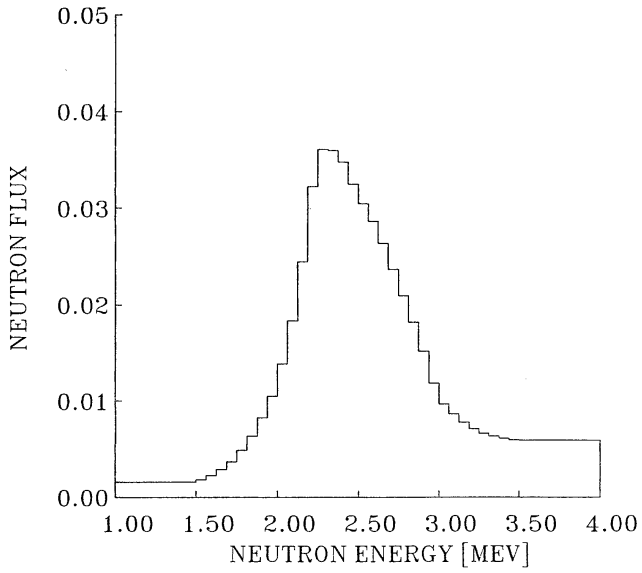

(a)

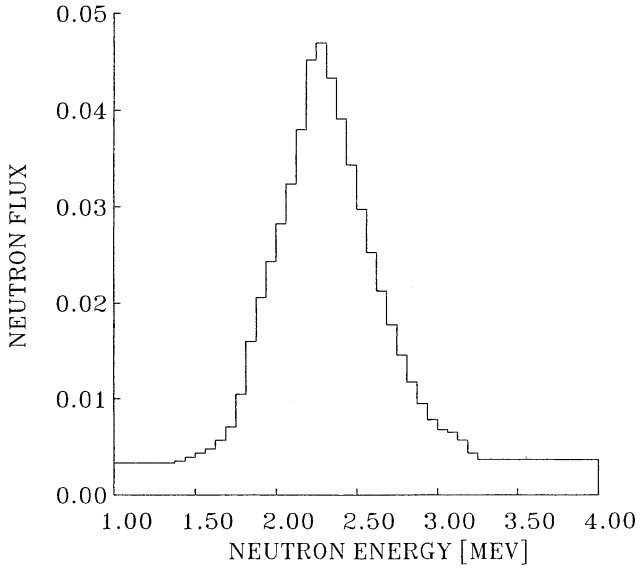

(b)

Figure 1. Neutron energy spectra derived from a maximum entropy unfolding of the knock-on proton track size distribution for detectors in the 145° (a) and the normal incidence (b) positions.

located behind the target at 20 cm and 145° to the target normal and figure 1(b) is that from detectors located at 20 cm and 0°. The spectra were integrated over six shots to improve the signal-to-noise ratio. The average intensity on target was 8×10^{18} W cm^{-2}. The spectral distributions have a quasi-Gaussian profile and both have an energy full width at half maximum (FWHM) of 680 keV. However, extensive calculations have shown that it is

possible to generate a Gaussian-type neutron distribution even from very non-Maxwellian ion velocity distributions and it is not possible to deduce a thermonuclear interpretation from the shape of the neutron spectra alone [12]. The neutron spectra have a systematic centring error of ± 100 keV (corresponding to an upper limit in the centre-of-mass motion of ± 8 keV) due to uncertainty in the proton track calibration in the CR-39. The spectra are centred at 2.3 MeV and 2.35 MeV for the forward and backward direction detectors, respectively, which is within the centring error of the technique for 2.45 MeV neutrons. Detectors located on the chamber wall at 55 cm from the target showed a signal 1/8 of the level of the main detectors, confirming a $1/R^2$ fall off from the chamber centre.

Although the CR-39 detectors have a limited spectral range, they are insensitive to γ-radiation. On the other hand, the current mode time-of-flight detectors (or *n*TOF) are sensitive to x-rays and gamma rays, although they do have a much larger spectral range. Each of the *n*TOF detectors was housed in a lead 'pig' to reduce this sensitivity. These pigs entirely enclosed each detector and provided at least 2.5 cm of Pb shielding to the sides and the back. The pig enclosure included 0.6 cm of Pb to the front of the detector; additional amounts were used in front and were varied from 2.5 to 12.5 cm during the course of the experiment. Despite this large amount of shielding, hard x-ray fluxes on these shots were so high that saturation of the *n*TOF detectors was a major problem. For some shots, the detectors saturated so badly that there was no charge available at neutron arrival time. For these shots the *n*TOF detectors could not even determine if neutrons were present. This problem was somewhat reduced when D_2 targets were irradiated due to the reduced bremsstrahlung emission generated during the interaction.

The signals from the cryogenically cooled D_2 target appear to divide into two categories, DD neutrons producing a relatively sharp peak at 2.45 MeV and multi-MeV neutrons with a broad energy distribution. The DD peak is observable mostly just on lower intensity shots. Figure 2 shows two signals for D_2 targets from the current mode time-of-flight detectors located at the normal incidence, 0° position at 1.18 m. The targets were irradiated at intensities of (a) 9×10^{17} W cm^{-2} and (b) 5×10^{18} W cm^{-2}. At intensities of 10^{18} W cm^{-2} on target, the d(d, n)^{3}He reaction appears with a maximum yield of $\sim 10^7$. This is illustrated in figure 2(a), where the 2.45 MeV peak is relatively sharp. As the intensity on target increases to 5×10^{18} W cm^{-2}, the time-of-flight signals broaden, and become anisotropic. This is illustrated in figure 2(b). Energy spectra, $P(E)\mathrm{d}E$, can also be produced from the time-of-flight signals. Shot 6021813 is one of the higher quality data points and its energy spectrum is shown in figure 3. In this case, both detectors were located at the normal incidence 0° position at 1.18 cm and 1.96 cm. Since the time spectra for most shots are similar, it can be concluded that this is a typical energy spectrum. The fact that both spectra in figure 3 are similar when the solid angles for the detectors are taken into account confirms the production of neutrons.

We will now analyse six possible generation mechanisms: (a) beam–heat shield ^{27}Al(d, n) reactions, (b) photodisintegration of deuterium, (c) late time γ-radiation, (d) thermonuclear and (e) beam–target-type processes, and finally (f) bulk plasma motions. The beam–heat shield ^{27}Al(d, n) reactions can produce a neutron energy spectra that contains lower energy neutrons for the D_2 target. However, similar yields were measured by the activation counters for both D_2 and C_8D_8 targets (the deuterium density is similar for both targets). This casts doubt on this process simply because the C_8D_8 targets clearly required no heat shield. Both the $1/R^2$ fall off in yield for the CR-39 neutron detectors and the time-of-flight spectra in figure 3 tend to rule out a beam–wall interaction process. The differences between the spectra for the two targets in figures 1 and 3 do tend to rule out photo-disintegration of deuterium by γ-radiation, as one would expect the lower neutron energy

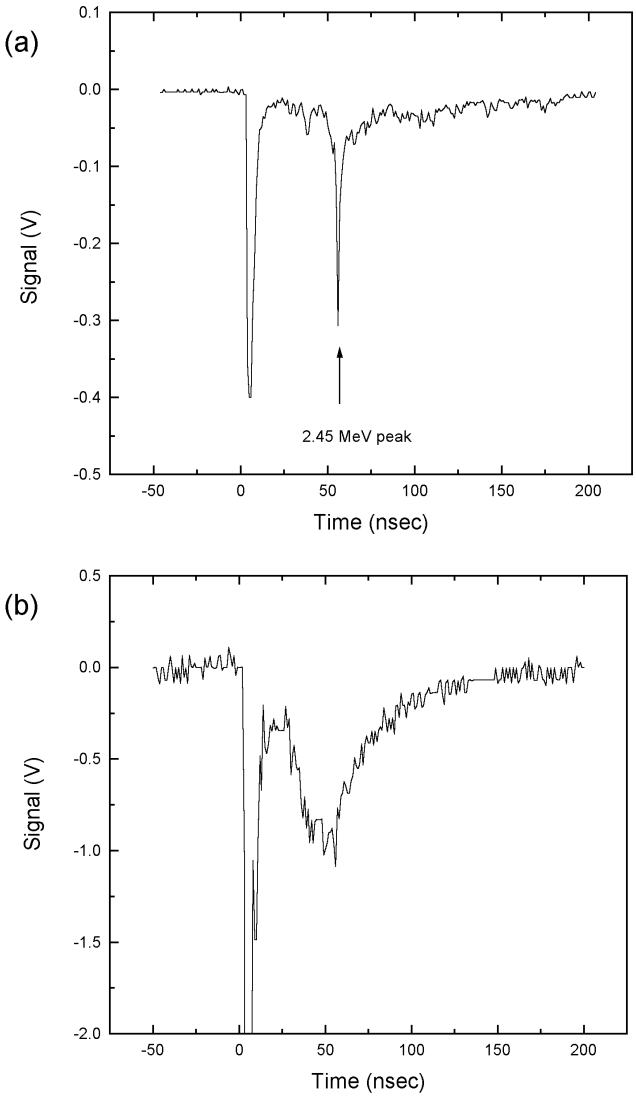

Figure 2. Time-of-flight signals for D_2 target irradiated at (a) 9×10^{17} W cm^{-2} and (b) 5×10^{18} W cm^{-2}.

component to increase for the deuterated plastic targets due to the increased bremsstrahlung emission resulting from the higher Z of the target material.

If late time γ-radiation is occurring over an extended period (which may be due to a succession of much lower intensity post pulses hitting the target), then this may register on the current mode time-of-flight detectors as a false lower energy component. This then leads us back to considering the neutron spectrum derived from the track detectors in figure 1. Here the neutron energy spectra strongly suggest their production by fusion of deuterium nuclei. Given the small Doppler shift and spectral width (680 keV from figure 1) the obvious hypothesis is that the neutrons originate in a thermonuclear plasma. If we hypothesize that: (i) the neutrons originate in a hemisphere (radius R) of uniformly heated solid density plasma

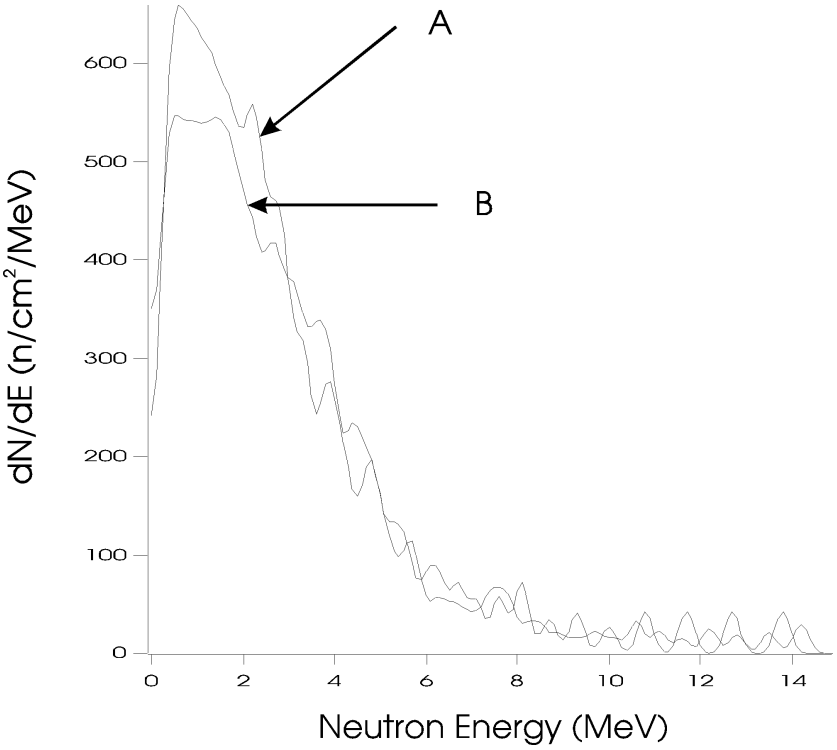

Figure 3. Neutron energy spectra $\mathrm{d}N/\mathrm{d}E$ derived from time-of-flight signals for detectors located in the normal incidence direction at distances of 1.18 m (A) and 1.96 m (B) for a D_2 target irradiated at 5×10^{18} W cm^{-2}.

(temperature T_{plasma}) centred on the middle of the laser spot, (ii) the electron deuteron and carbon temperatures are equal, (iii) the laser energy absorbed in this plasma is E_{absorbed} and (iv) fusion reactions occur during the time for hydrodynamic expansion $\tau_{\mathrm{hydro}} \sim R/c_{\mathrm{sound}}$ where c_{sound} is the isothermal sound speed then the neutron yield should be

$$N \approx \left(\frac{E_{\mathrm{absorbed}}}{10\ \mathrm{J}}\right)^{4/3} \left(\frac{T_{\mathrm{plasma}}}{30\ \mathrm{keV}}\right)^{-7/12} 1.4 \times 10^{8} \qquad (1)$$

where the approximation has been made that the neutron production rate is proportional to $T^{5/4}$ in the range of interest. If $T_{\mathrm{plasma}} = 30$ keV and $E_{\mathrm{absorbed}} = 10$ J (which is reasonable given the 40–60% absorption fractions inferred from the experiments of Beg *et al* [7] and Zepf *et al* [13]) then the radius of the plasma is $R = 10$ μm and the expansion time is $\tau_{\mathrm{hydro}} \sim 8$ ps. The temperature dependence is relatively weak and a low value is indicated by the large neutron yield, but T_{plasma} cannot be much less than 30 keV because the fusion rate drops of rapidly below 20 keV and the neutron spectra imply a temperature closer to 70 keV [12]. Hence a thermonuclear interpretation cannot easily explain the large neutron yield. Further reasons for rejecting the thermonuclear interpretation are that: (i) the Coulomb mean free path for 400 keV fast electrons generated at intensities of 10^{19} W cm^{-2} [7] is vastly greater than the 10 μm radius in which the energy must be deposited to heat the plasma to thermonuclear temperatures, (ii) a thermonuclear plasma is not easily established because the collisional equilibration time is many hundreds of ps, (iii) the cooling time of a 30 keV plasma of 10 μm radius due to electron thermal conduction is less than 0.1 ps.

We now analyse the possibility that a beam–target-type interaction could produce up to 7×10^7 neutrons/sr, as a result of hole boring [14]. In the case of hole boring, electrons are accelerated into the target as a result of resonance absorption, $\boldsymbol{v} \times \boldsymbol{B}$ or vacuum heating. This sets up an electrostatic field due to charge separation which accelerates the ions into the target. The electron density is seven times the deuteron density. If the absorbed laser energy of 10 J were divided in this proportion between electrons and deuterons and the deuterons were heated to 100 keV (the minimum for efficient neutron production, in keeping with the ion measurements and possibly arising from the electrostatic fields around the target surface) then the number of energetic deuterons would be 8×10^{13}. The neutron generation cross section and the Coulomb cross section for energy loss to cold background carbon ions, deuterons and electrons (multiplied by n_e/n_D to allow for their larger number density) are: $\sigma_{fusion} = 1.7 \times 10^{-30}$ m^2; $\sigma_{DC} = 4 \times 10^{-26}$ m^{-2}; $\sigma_{DD} = 7 \times 10^{-27}$ m^{-2}; and $(n_e/n_D)\sigma_{De} = (T_e/\text{keV})^{-3/2}\, 8 \times 10^{-25}$ m^2. The Coulomb cross sections are derived from Nishikawa and Wakatani [15] for relaxation of a 100 keV Maxwellian distribution of deuterons with $\log \Lambda = 5$. If the electron temperature is greater than 7 keV, the energetic deuterons lose their energy predominantly to background carbon ions. The ratio of the neutron production to the Coulomb cross section is 4×10^{-5}, so the expected neutron yield would be 2.4×10^8 neutrons/sr which is close to the largest observed yield. If the electron temperature is less than 7 keV, the Coulomb cross section is greater and the neutron yield is less by $(T_e/7\ \text{keV})^{3/2}$. However, an electron temperature of 7 keV or greater is not unreasonable since the deuterons themselves would heat the plasma as they lost energy. If the energy of the energetic deuterons were greater than 100 keV, the fusion cross section would be greater and the Coulomb cross section less, favouring an increased neutron production. Can the deuteron energy be much less than 100 keV? Slaughter [12] has shown that a Maxwellian ion distribution produces a neutron spectral width which is identical to that produced by a monoenergetic deuteron beam with a mean energy two to four times higher. The 680 keV spectral width from figure 1 implies a 70 keV temperature if the distribution is Maxwellian. Consequently, the deuteron beam cannot have an energy much less than ~100 keV and still be consistent with the observed spectra. We therefore conclude that a beam–target-type interaction is energetically feasible, but requires efficient transfer of energy to the deuterons, which is not easily explained, but might result from the electrostatic fields around the target surface.

The isotropy and lack of systematic Doppler shift in figure 1 for C_8D_8 targets may be taken to imply a thermonuclear origin, but this can equally be explained if the energetic deuterons were produced with some degree of isotropization, or were isotropized by angular scattering off of the carbon ions. Indeed, the cross section for isotropization by angular scattering is about six (the carbon-to-deuteron mass ratio) times greater than the Coulomb scattering cross section energy for energy loss to background carbon ions. Thus, a relatively isotropic deuteron, and therefore neutron, distribution would be expected.

Another possible explanation for the observed spectra in figure 3 is that of bulk plasma motion, which can also produce much lower energy neutrons. Suppose that energetic ions are either directed into the target as a result hole boring or are away from the target in the blow-off plasma. When considering either case, transfer to the plasma flow frame of reference. Let these deuterons have a Maxwellian distribution, and, for the moment, neglect collisions with the stationary deuterons of the background plasma (the beam–target-type process discussed above). These deuterons can interact with each other via 'transverse' collisions at relatively low velocities. These collisions produce neutrons with an energy that is close to 2.45 MeV in the centre-of-mass frame of reference. When transformed back to the laboratory frame, significant shifts in neutron energies occur. The fact that the CR-39

neutron detectors do not register many lower energy neutrons for the C_8D_8 case does suggest that there may be differences in the ion dynamics for pure deuterium targets compared with deuterated plastic targets.

In conclusion, we have presented the first observations of high neutron fluxes when deuterated targets were irradiated with 1054 nm, picosecond laser pulses of 8–20 J at intensities approaching 10^{19} W cm^{-2}. At lower intensities, the d(d, n)^{3}He reaction is observed with yields of $\sim 10^7$. As the intensity increases, yields of up to 7×10^7 neutrons/sr are obtained. Our analysis has shown that a thermonuclear source for these higher yield neutrons is unlikely, but a beam–target interpretation is energetically feasible. Distinguishing between the beam–target and bulk plasma motion processes from the observed neutron spectra for the different target materials will be the subject of further investigation. We believe the results presented here suggest that energy deposition from fast ions may play a significant role in the fast ignition scheme for ICF.

The authors gratefully acknowledge the support of the staff of the Central Laser Facility of the Rutherford Appleton Laboratory (especially Tony Damerell, Steve Angood and Andy Frackiewicz) without whose assistance this work would not have been possible. The work was supported by the United Kingdom Engineering and Physical Sciences Research Council.

References

[1] Tabak M, Hammer J E, Glinsky M E, Kruer W L, Wilks S C, Woodworth J, Campbell E M, Perry M and Mason R J 1994 *Phys. Plasmas* **1** 1626
[2] Hares J D, Kilkenny J, Key M H and Lunney J G 1979 *Phys. Rev. Lett.* **42** 1216
[3] Pearlman J S and Morse R L 1978 *Phys. Rev. Lett.* **40** 1625
[4] Wilks S C, Kruer W L, Tabak M and Langdon A B 1992 *Phys. Rev. Lett.* **69** 1383
[5] McCall G H, Young F, Ehler A W, Kephart J F and Godwin R P 1973 *Phys. Rev. Lett.* **30** 1116
[6] Fews A P, Norreys P A, Beg F N, Bell A R, Dangor A E, Danson C N, Lee P and Rose S J 1994 *Phys. Rev. Lett.* **73** 1801
[7] Beg F N, Bell A R, Dangor A E, Danson C N, Fews A P, Glinsky M E, Hammel B A, Lee P, Norreys P A and Tatarakis M 1997 *Phys. Plasmas* **4** 447
[8] Danson C N *et al* 1993 *Opt. Commun.* **103** 392
[9] Cable M D and Nelson N B 1988 *Rev. Sci. Instrum.* **59** 1738
[10] Fews A P and Henshaw D L 1982 *Nucl. Instrum. Methods* **197** 512
[11] Fews A P, Lamb M J and Savage M 1992 *Opt. Commun.* **94** 259
[12] Slaughter D R 1989 *Rev. Sci. Instrum.* **60** 552
[13] Zepf M *et al* 1996 *Phys. Plasmas* **3** 3242
[14] Kruer W L and Wilks S C 1992 *Plasma Phys. Control. Fusion* **34** 2061
[15] Nishikawa K and Wakatani M 1994 *Plasma Physics* (Berlin: Springer)